Traveling Wave-Based Hybrid Line Faulted Section Detection: A Practical Approach

Felipe V. Lopes, Eduardo Jorge S. Leite Jr., Flávio B. Costa, Washington L. A. Neves

Abstract—This paper presents the practical application of a traveling wave (TW)-based algorithm for faulted section detection on hybrid transmission lines (HTLs). It analyzes fault-induced wavefronts at both line terminals, requiring the detection of the first incident TWs only. The presented formulation can be applied in HTLs with any number of sections irrespective of their electrical parameters, provided that the arrival times of the first incident TWs at both line ends are properly detected. Only the propagation times of the HTL sections are required to be known, which in turn can be calculated from the line electrical parameters or estimated during line energization maneuvers. A practical approach of the presented algorithm is demonstrated by means of Alternative Transients Program (ATP) simulations and Excel© application examples, considering fault scenarios in a multi-section 380 kV/50 Hz HTL. The obtained results reveal that the algorithm is straightforward, generalist and reliable.

Keywords—ATP, faulted section detection, hybrid transmission lines, traveling waves, power systems.

I. Introduction

THE GROWING demand for electric energy has imposed several technical and operational challenges for utilities, specially regarding the transmission networks, which are requested to transmit power safely and reliably over a diversity of terrains, passing through populated areas or even by rivers and lakes. As a result, a number of power transmission solutions have been considered to guarantee a reliable delivery of electrical energy to consumer centers, without violating environmental and technical restrictions that often arise along the area where the line is installed. Among these solutions, the use of power transmission paths formed by the combination of sections with different electrical parameters has been a common practice, such as those which combine overhead lines (OLs), underground cable lines (ULs) and submarine cable lines (SLs), or even those formed by conductor sections of the same nature but with different electrical parameters, as the case of series OLs installed on different towers [1], [2]. This kind of non-homogeneous lines are called hybrid transmission lines, which are referred here as HTLs.

Felipe Lopes and Eduardo Leite Jr. are with the Department of Electrical Engineering at University of Brasília (UnB), 70910-900 Brasília-DF, Brazil. (e-mail: felipevlopes@ene.unb.br, eduardoleitejr@gmail.com).

Flávio B. Costa is with the School of Science and Technology at Federal University of Rio Grande do Norte (UFRN), Natal 59.078-970, Brazil (e-mail: flaviocosta@ect.ufrn.br).

Washington L. A. Neves is with the Department of Electrical Engineering of Federal University of Campina Grande (UFCG) (e-mail: waneves@dee.ufcg.edu.br).

When a fault occurs on HTLs, one of the most challenging and important task is to identify the faulted section [3]. It becomes even more relevant for HTLs formed by OLs, ULs and SLs, because if the fault takes place within UL or SL sections, it is probably a permanent fault, thereby auto-reclosing schemes must be blocked to avoid further cable deterioration and the disturbance spread on the electrical power system [4]. However, most traditional transmission line fault locators, protective relays and disturbance diagnosis computer programs are usually designed to operate in homogeneous systems, considering an uniform distribution of the electrical parameters along the transmission line length [5]. Thus, several researchers have made efforts to develop disturbance diagnosis algorithms for HTLs, specially toward finding solutions for faulted section detection.

In the open literature, there are works which address the HTL faulted section detection problem [3], [6], [7], but most solutions are focused only on the two-section HTL case. As an exception, algorithms for multi-section HTLs are reported in [4], [8]. The one presented in [4] is available in an actual protective device [9]. However, although it has been successfully applied in real-world fault scenarios, its application is limited in practice to HTLs with five sections in order to overcome problems due to attenuation of fault-induced TWs [9], especially when the HTL contains UL and SL sections. Hence, although the referred algorithm could be generalized for any number of sections, its practical application in HTLs with more than five sections would be a problem for utilities, since they would have to implement their own computational routines or adapt existing ones.

In the near future, it is expected to see more multi-section HTLs in operation, so that the development of generalist and practical faulted section detection methodologies able to operate in HTLs with any number of sections has attracted the interest of utilities. Thus, in this paper, a TW-based faulted section detection algorithm for multi-section HTLs is presented, and its practical application is demonstrated. It only requires the detection of the first incident TWs at both line ends, and the knowledge of the travel time of each HTL section, which can be estimated from the line parameters (if they are available) or from energization maneuvers [4]. The practical algorithm application is demonstrated by means of ATP simulations, considering fault scenarios in a multi-section 380 kV/50 Hz HTL. The obtained ATP records are played back in actual TW-based protective relays, from which synchronized TW filtered signals are obtained. Also, to make the algorithm attractive for practical procedures, it is demonstrated how an Excel© worksheet could be used to apply the algorithm.

II. IDENTIFYING THE HYBRID LINE FAULTED SECTION

To facilitate the algorithm understanding, Fig. 1 depicts TWs propagating along a multi-section HTL with N sections. As mentioned earlier, the HTL faulted section detection algorithm requires only the identification of the first incident TWs arrival times at local and remote HTL terminals, which will be referred to hereafter as t_L and t_R, respectively. Therefore, being T_ℓ the HTL total propagation time and t_0 the fault inception time, one can observe that:

$$(t_R - t_0) = T_\ell - (t_L - t_0) . \tag{1}$$

From the literature, the classical two-terminal fault location procedure analyzes the time difference $t_R - t_L$ to calculate the fault distance. Based on the same concept, from the instants t_R, t_L and t_0, it is derived that:

$$t_R - t_L = T_\ell - 2(t_L - t_0) . \tag{2}$$

Irrespectively on the point on the HTL the fault takes place, if it is within the n-th HTL section, $t_L - t_0$ will be greater than or equal to the total travel time computed for the first $(n-1)$ sections upstream the faulted one. As a result, if a fault occurs at the beginning of a given n-th section, close to the junction point between the sections $n-1$ and n, one can obtain that:

$$t_L - t_0 = \sum_{q=1}^{n-1} \tau_q , \tag{3}$$

where τ_q is the propagation time of the q-th HTL section.

Finally, substituting (3) in (2), the time difference $t_R - t_L$ for a given fault within the n-th section at the junction point between the sections $n-1$ and n is obtained, which will be represented hereafter by $t_{R,n} - t_{L,n}$, being:

$$t_{R,n} - t_{L,n} = T_\ell - 2 \left[\sum_{q=1}^{n-1} \tau_q \right] . \tag{4}$$

From the analysis presented so far, it is noticed that there are expected values for $t_{R,n} - t_{L,n}$ that can be calculated for each junction point between two consecutive HTL sections. For a HTL with N sections, for instance, $N-1$ junction points are verified, being the first one located at the end of Section 1 and the $(N-1)$-th junction point located at the beginning of

the N-th HTL section (last section). Thus, the time difference $t_R - t_L$ calculated from the TW detection procedure at both HTL terminals can be compared with the expected values of $t_{R,n} - t_{L,n}$ for each HTL junction point. Therefore, by varying n from 1 to N, the faulted section is detected by means of the following condition:

$$t_{R,n} - t_{L,n} \geq t_R - t_L \geq t_{R,n+1} - t_{L,n+1} , \tag{5}$$

which can be represented by:

$$T_\ell - 2 \left[\sum_{q=1}^{n-1} \tau_q \right] \geq t_R - t_L \geq T_\ell - 2 \left[\sum_{q=1}^{n} \tau_q \right] . \tag{6}$$

In practice, only one value of n will satisfy (6), which represents the section number within which the fault is.

III. PRACTICAL APPLICATION OF THE PROPOSED HTL FAULTED-SECTION DETECTION METHODOLOGY

In practice, the need for implementing computational routines (especially filtering techniques) to apply a given protection or fault location algorithm is often reported by utilities as undesirable. Therefore, understanding this issue, a practical approach of the presented algorithm is described in this section, providing guidelines on how an engineer can apply condition (6) in practical real-world cases. To do so, commercially available computer programs are suggested, through which the step-by-step of the faulted-section detection algorithm can be accomplished.

To demonstrate the algorithm application, the seven-section 380 kV/50 Hz HTL shown in Fig. 2 is evaluated. It will be also used in the ATP simulations analyzed in the next sections, where four different fault points are considered (F1, F2, F3 and F4). Such a HTL is composed by four OL sections 12 km long, two UL sections 5 km long and one SL section 3.7 km long, which were randomly arranged over the HTL. All sections were modeled using the frequency-dependent JMartí model, being the electrical parameters taken from the literature [2], [10], [11], resulting in $T_{OL} = 40.6$ μs, $T_{UL} = 25.9$ μs and $T_{SL} = 19.9$ μs, where T_{OL}, T_{UL} and T_{SL} are the propagation times of the OL, UL and SL sections, respectively. Thus, from the number of each section type and their propagation times, the HTL total travel time $T_\ell = 234.1$ μs is obtained.
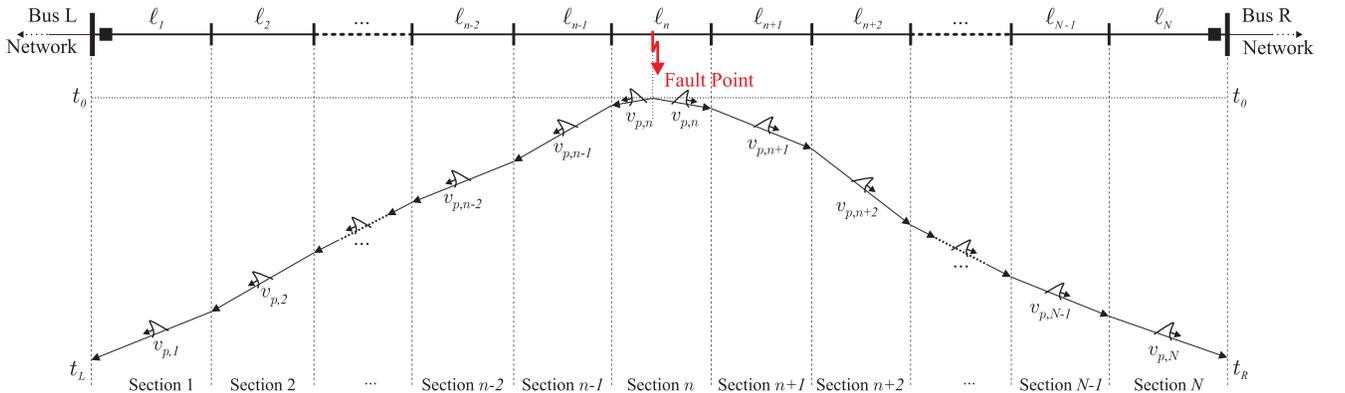
Fig. 1. Bewley diagram for fault within the n-th section.
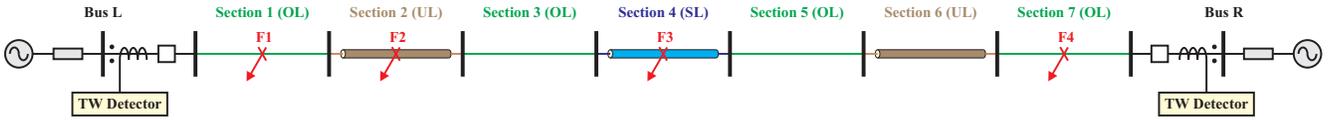
Fig. 2. Test seven-section 380 kV/50 Hz HTL.

In this paper, the analyzed HTL faulted section detection procedure is divided into two steps: 1) Detection of the first incident TWs which arrive at both HTL terminals; and 2) HTL faulted section detection. Thus, with the aim to make the proposed methodology attractive for utilities, both algorithm steps are performed here by using commercially available protective devices and computer programs as described next.

A. Step 1: Detection of the First Incident TWs

To extract TW information from the fault-induced transient signals at both HTL ends, digital filters available in the SEL-T400L relay are applied in this paper [9]. It is worthy to emphasize that the filtering procedure could be implemented in any mathematical computational tool, but actual relays were used to obtain a more realistic testing scheme. The used relays apply the Differentiator-Smoother filter, which has unitary gain, responding to step- and ramp-changes in the input signals with triangle- and parabola-shaped outputs, respectively, whose peaks can be associated to the sought TW arrival times [12]. Unfortunately, the thresholds are factory-selected in the relay, thereby it is difficult to properly detect overdamped transients induced by faults on HTLs. It is probably why the SEL-T400L limits its fault location applications to HTLs with a maximum of five sections. However, the goal here is to analyze multi-section HTLs with more than five sections, so that the detection of the first incident TWs is manually performed rather than considering the arrival times automatically estimated by the device. As a result, SEL-T400L is used only to generate comtrade files of the TW filtered signals, which are then externally analyzed.

Once the TW filtered signals are taken from SEL-T400L relays, it is suggested to analyze them using the SynchroWAVe software [13]. Basically, assuming that the comtrade files taken from both HTL ends are synchronized, the TW filtered signals should be loaded together in SynchroWAVe and, then, the available cursors must be aligned with the first peaks verified in each signal, which represent the first incident TWs at the line terminals. By doing so, the absolute value of the time difference between the two cursors will automatically be displayed, representing $|t_R - t_L|$, as shown in Fig. 3. Thus, the time difference $\kappa \cdot |t_R - t_L|$ should be considered, being $\kappa = 1$ or $\kappa = -1$ whether the first TW detection occurs at local or remote line terminals, respectively.

After the time difference $t_R - t_L$ has been calculated, we proceed to the second step, in which condition (6) is analyzed. Aiming to make the algorithm attractive for utilities, the use of an Excel© worksheet is suggested, through which the time difference $t_R - t_L$ can be easily analyzed overcoming the need for complicated computational procedures.
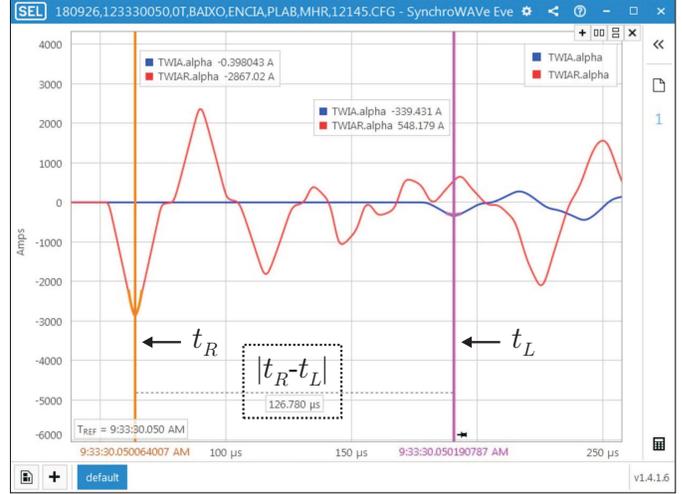
Fig. 3. Time difference $t_R - t_L$ calculation using the SynchroWAVe software.

B. Step 2: HTL Faulted Section Detection

In this paper, the main goal is to show a practical way to accomplish the HTL faulted-section detection by using traditional computational programs. As mentioned before, here, the Excel© program is applied to create a worksheet that receives as input the time difference $t_R - t_L$ and the HTL topology, being able to automatically calculate all the other variables required to analyze the condition (6), from which the HTL faulted section is detected. Here, the Excel© program was chosen because it is widely used by utilities in a number of applications, so that it is expected that professionals are familiar with this mathematical platform.

Fig. 4 illustrates the worksheet that has been implemented to apply the HTL faulted section detection, where yellow cells are the input cells and the blue cells are those which display intermediate results. Further details on the created worksheet can be found in the Appendix.

It should be pointed out that the suggested implementation described in this section is not the only way to analyze condition (6). As mentioned earlier, the goal here is to demonstrate how the studied HTL faulted section detection algorithm could be applied in real-world fault cases, in a simple way, by using well-known and familiar computer programs, overcoming the need for complicated codes or knowledge on computer programming languages. Obviously, other optimized implementations could be developed, but the presented worksheet is enough to proceed with the detection of faulted sections on HTLs, which can be easily adapted to HTLs with any number of sections.

Fig. 4. Excel© worksheet to apply the studied algorithm.

Fig. 5. Step-by-step of the algorithm evaluation procedure.

IV. ALGORITHM PRACTICAL APPLICATION

Here, the practical application of the proposed algorithm is demonstrated. It is evaluated through ATP simulations of faults on the HTL shown in Fig. 2. Due to space limitations, only phase A-to-ground (AG) fault cases were analyzed: Case 1) Fault F1 within Section 1 (OL section) at 30% of ℓ_1=12 km; Case 2) Fault F2 within section 2 (UL section) at 80% of ℓ_2=5 km; Case 3) Fault F3 within section 4 (SL section) at 50% of ℓ_4=3.7 km; Case 4) Fault F4 within section 7 (OL section) at 10% of ℓ_7=12 km, where ℓ_n is the length of the n-th faulted section. As the automatic transient detection procedure is not evaluated in this paper, noise-free signals were considered.

Fig. 5 shows the algorithm evaluation procedure step-by-step. To illustrate its practical application, the obtained ATP records were played back in two SEL-T400L relays, between which an optical fiber cable was used to synchronize their clocks. The fault record playback was carried out using an innovative test function available in SEL-T400L relays, which allows simulated comtrade files sampled at 1 MHz to be loaded in the protective device memory in .ply format and then played back [9], [14], overcoming the need for test boxes, which usually have analog outputs with limited frequency bandwidth. Thus, as shown in Fig. 5, each evaluated fault case was firstly simulated in ATP considering a time-step equal to 1 μs, generating comtrade files, which were converted to .ply files via SEL AcSELerator Quickset. Then, the .ply files were loaded and played back in the SEL-T400L relays generating the TW filtered signals via Differentiator-Smoother filter, which were analyzed using the SynchroWAVe software [13] to calculate $t_R - t_L$. Finally, the estimated $t_R - t_L$ value was loaded in the proposed Excel© worksheet, through which the HTL faulted section was automatically identified.

A. Case 1: Fault within Section 1 at 30% of ℓ_1=12 km

In Case 1, an AG fault within Section 1 (OL section) at 30% of ℓ_1 was taken into account, which represents a total distance from the local terminal equal to 3.6 km. Fig. 6 shows the TW filtered signals taken from both local and remote relays, from which $|t_R - t_L| = 209.341$ μs was obtained. Thus, since $t_L < t_R$, $\kappa = 1$ is used, thereby $t_R - t_L$ is taken as 209.341 μs. Finally, using the estimated $t_R - t_L$ value in the Excel© worksheet, a fault within Section 1 was detected, as expected, as shown in Fig. 6.
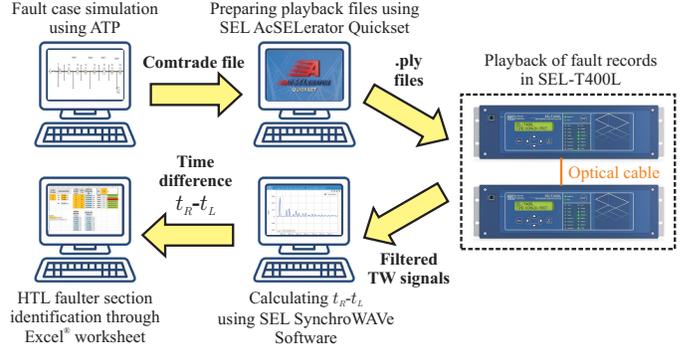
B. Case 2: Fault within Section 2 at 80% of ℓ_2=5 km

Case 2 is related to an AG fault within Section 2 (UL section) at 80% of ℓ_2. It results in a total distance from the reference local bus equal to $\ell_1 + 0.8 \cdot \ell_2 = 12 + 0.8 \cdot 5 = 16$ km. Local and remote TW filtered signals obtained from SEL-T400L relays are depicted Fig. 7. In this case, $|t_R - t_L| = 110.176$ μs was obtained, as shown in Fig. 7. Since $t_L < t_R$, $\kappa = 1$ is considered, resulting in $t_R - t_L = 110.176$ μs. Using this value in the proposed Excel© worksheet, a fault within Section 2 was detected, as expected.

C. Case 3: Fault within Section 4 at 50% of ℓ_4=3.7 km

Case 3 illustrates the waveforms obtained during an AG fault at the middle of Section 4 (SL section). It represents a total distance between the local reference terminal and the fault point equal to $\ell_1 + \ell_2 + \ell_3 + 0.5 \cdot \ell_4 = 12 + 5 + 12 + 0.5 \cdot 3.7 = 30.85$ km. TW filtered signals taken from the evaluated relays are shown in Fig. 8, from which $|t_R - t_L| = 0$ s was obtained. Thus, using $t_R - t_L = 0$ s in the proposed Excel© worksheet, a fault within Section 4 is indicated, as expected.

It should be noted that, coincidentally, even arranging the sections randomly in the HTL, the test power system became symmetrical around Section 4, in such a way that $t_R = t_L$, i.e., the TW detection errors at both line ends are canceled when $t_R - t_L$ is calculated. However, even if the system were asymmetrical around the HTL central section, (6) would adapt itself to the power system topology, guaranteeing the correct HTL faulted section detection.

D. Case 4: Fault within Section 7 at 10% of ℓ_7=12 km

Case 4 shows an AG fault within Section 7 (OL section) at 10% of ℓ_7, representing the case of a fault close to a junction point between two-consecutive HTL sections. In this case, the total fault distance from the reference local terminal is equal to $\ell_1 + \ell_2 + \ell_3 + \ell_4 + \ell_5 + \ell_6 + 0.1 \cdot \ell_7 = 12 + 5 + 12 + 3.7 + 12 + 5 + 0.1 \cdot 12 = 50.90$ km. Fig. 9 depicts the TW filtered signals taken from the evaluated SEL-T400L relays, through which $|t_R - t_L| = 161.374$ μs was calculated. Therefore, since in this case the first detection occurs at the remote line terminal, i.e., $t_L > t_R$, $\kappa = -1$ is considered, thereby $t_R - t_L = -161.374$ μs is obtained. Finally, applying the estimated $t_R - t_L$ value in the proposed Excel© worksheet, a fault within Section 7 was detected, as expected.
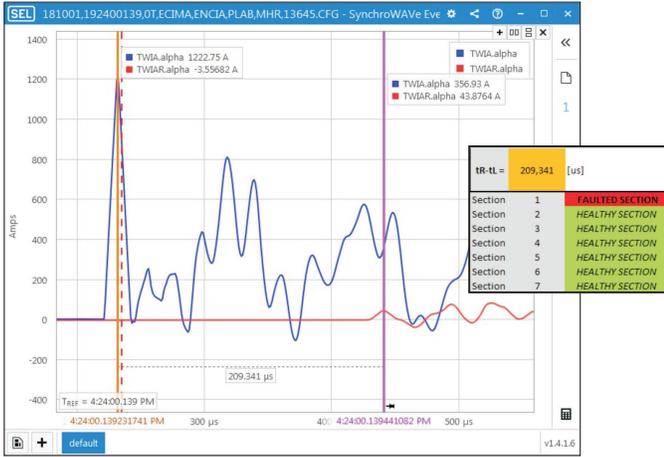
Fig. 6. Obtained results in Case 1: Fault within Section 1 at 30% of ℓ_1.
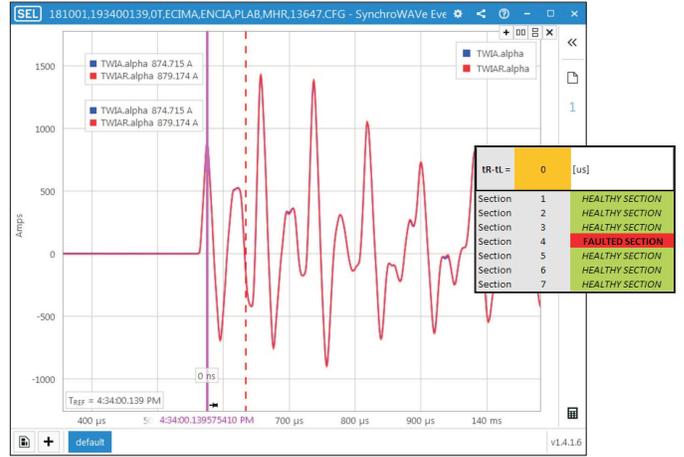
Fig. 8. Obtained results in Case 3: Fault within Section 4 at 50% of ℓ_4.

Fig. 7. Obtained results in Case 2: Fault within Section 2 at 80% of ℓ_2.
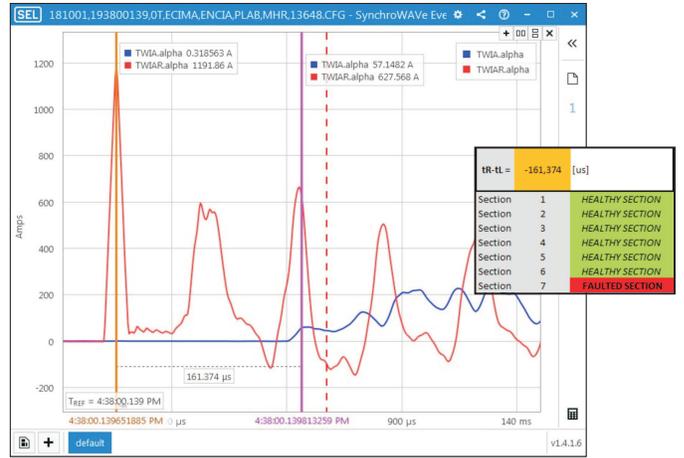
Fig. 9. Obtained results in Case 4: Fault within Section 4 at 10% of ℓ_7.

E. Additional Remarks

From the analyzed cases, it was demonstrated that the proposed algorithm is easy to apply and reliable. It properly detected the HTL faulted section in all evaluated fault scenarios, even in cases of faults close to HTL junction points. Even so, there are some issues regarding the features of fault-induced TWs that must be highlighted in order to alert engineers about difficulties that may be faced during the analysis of TW filtered signals.

From Figs. 6 to 9, the line end closest to the fault point presents TWs stronger than those measured at the farthest line end. Since UL and SL sections are usually short, TWs are expected to be also detectable in other scenarios, except in cases of very long UL and SL sections, when severe transient attenuation may occur. Besides, a lot of oscillations can be observed in TW filtered signals, which are the result of reflections at the HTL junction points. Sometimes, it may confuse the engineering crew, which can be led to align the time cursors with the signal peak that presents the greatest amplitude among those in the first few fault instants, which are not necessarily those related to the first

incident TWs at the monitored line terminals. The authors alert that it is not correct, in such a way the Synchrowave time cursors must be aligned with the first peak that show up in TW filtered signals, irrespectively of their amplitude. In fact, most TW fault recorders and TW-based protective devices will not properly detect these attenuated transients by using automatic TW detection approaches, since they normally consider conservative factory-selected thresholds. However, TW records can be evaluated manually, as proposed in this paper, guaranteeing a reliable HTL fault detection.

V. CONCLUSION

In this paper, a HTL faulted section detection algorithm was presented and tested. Its practical approach was also pointed out, through the demonstration of the algorithm application by using commercially available protective devices and computer programs. Basically, the algorithm requires only the synchronized detection of the first incident TWs at both HTL terminals, and the knowledge of the propagation time of each section, through which the system topology is mapped into a generalist condition that allows the proper HTL faulted section identification in multi-section systems.

To demonstrate the practical application of the proposed algorithm, SEL-T400L relays were used to extract TW information from the fault-induced transients. Then, the time difference between the first transient detections at both HTL ends was estimated through the Synchrowave software and, finally, an Excel© worksheet was proposed to apply the algorithm conditions. All guidelines to implement the referred worksheet were provided in order to make the algorithm attractive for utilities. Four fault cases in a seven-section 380 kV/50 Hz HTL were analyzed to evaluate the proposed algorithm and to demonstrate its practical application. The proposed algorithm showed to be reliable and easy-to-use, properly detecting the HTL faulted section in all evaluated scenarios.

APPENDIX

This appendix presents details on the implementation of the Excel© worksheet shown in Fig. 4. Since the test HTL shown in Fig. 2 has three types of sections (i.e., OL, UL or SL sections), their respective types and propagation times (represented by TOL, TUL or TSL in the worksheet) are informed in columns 'A' and 'C', lines 2-4. Then, in columns 'F' and 'G', lines 2-8 are created to represent the number and type of each section of the monitored HTL, so that the number of worksheet lines to be created should be equal to the number of sections in the monitored HTL. On the right side, in blue color, the cells in column 'H' must automatically read the associated propagation times taken from column 'C', organizing the sequence in which each section appears in the HTL. To do so, write in cell 'H2' the command:

```
=IF(G2=$A$2;$C$2;IF(G2=$A$3;$C$3;...
...IF(G2=$A$4;$C$4;"Invalid Code")))
```

and then drag the paintbrush across the other lines until the cell that represents the last HTL section.

To facilitate the application of (6), lines 11-17 in columns 'F' and 'H' are created to display the expected superior and inferior limits that should be taken into account during the analysis of the time difference $t_R - t_L$. In these columns, the left and right side sums shown in (6) are automatically calculated, based on the sequence of sections previously informed in columns 'F' and 'G', lines 2-8. In this paper, the cell 'F11' was separately programmed, because the sum does not exist in the superior limit in cases of $n = 1$. Therefore, the command "=($C$6-2*0)" is suggested to be firstly written in cell 'F11'. Then, write in cell 'F12' the command:

```
=($C$6-2*SUM($H$2:H2))
```

and then drag the paintbrush across the remaining blue lines. Similarly, write in cell 'H11' the command:

```
=($C$6-2*SUM($H$2:H2))
```

and then drag the paintbrush across the other blue lines related to the inferior time limit values. The worksheet user should pay attention to the total HTL travel time and the individual travel times, which must be represented in the same time unit. Here, all time variables are represented in microseconds.

In cell 'L1', the $t_R - t_L$ value is informed in microseconds to the worksheet and, below, lines 2-8 are programmed to show the section number previously defined in column 'F'. In column 'M', lines 2-8, conditional cells indicate the HTL faulted section. As an additional feature of the created worksheet, the red color will appear indicating a 'Faulted Section' whether $t_R - t_L$ is in between the inferior and superior values displayed in columns 'F' and 'H', lines 11-17, otherwise, the green color will appear, indicating a 'Healthy Section'. To do so, write in cell 'M2' the command:

```
=IF(AND($L$1<=F11;$L$1>=H11);...
..."FAULTED SECTION";"HEALTHY SECTION")
```

and then drag the paintbrush across the remaining lines. Finally, create a rule on these cells to make them to appear in red and green color in cases of 'Faulted Section' and 'Healthy Section', respectively.

REFERENCES

[1] M. Bawart, M. Marzinotto, and G. Mazzanti, "Diagnosis and location of faults in submarine power cables," *IEEE Electrical Insulation Magazine*, vol. 32, no. 4, pp. 24–37, July 2016.

[2] J. Vargas, A. Guzmán, and J. Robles, "Underground/submarine cable protection using a negative-sequence directional comparison scheme," in *26th Annual Western Protective Relay Conference*, Oct 1999.

[3] C. F. Jensen, *Online Location of Faults on AC Cables in Underground Transmission Systems*, 1st ed. Aalborg, Denmark: Springer International Publishing, 2014.

[4] B. Kasztenny, A. Guzmán, M. V. Mynam, and T. Joshi, "Locating faults before the breaker opens - adaptive autoreclosing based on the location of the fault," in *71st Annual Conference for Protective Relay Engineers*, Mar 2018.

[5] M. M. Saha, J. Izykowski, and E. Rosolowski, *Fault Location on Power Networks*, ser. Power Systems. London: Ed. Springer, 2010.

[6] E. J. S. Leite and F. V. Lopes, "Traveling wave-based fault location formulation for hybrid lines with two sections," in *2017 Workshop on Communication Networks and Power Systems (WCNPS)*, Nov 2017, pp. 1–4.

[7] Ö. Altay, E. Gürsoy, A. Font, and Ö. Kalenderli, "Travelling wave fault location on hybrid power lines," in *2016 IEEE International Conference on High Voltage Engineering and Application*, Sept 2016, pp. 1–4.

[8] O. M. K. K. Nanayakkara, A. D. Rajapakse, and R. Wachal, "Location of dc line faults in conventional hvdc systems with segments of cables and overhead lines using terminal measurements," *IEEE Transactions on Power Delivery*, vol. 27, no. 1, pp. 279–288, Jan 2012.

[9] *SEL-T400L Ultra-High-Speed Transmission Line Relay Traveling-Wave Fault Locator High-Resolution Event Recorder.*, Schweitzer Engineering Laboratories, 2018. [Online]. Available: https://selinc.com/products/T400L/

[10] L. Colla, F. M. Gatta, A. Geri, and S. Lauria, "Lightning overvoltages in hv-ehv mixed overhead-cable lines," in *2017 International Conference on Power Systems Transients (IPST'07)*, Jun 2017.

[11] J. R. Marti, "Accurate modelling of frequency-dependent transmission lines in electromagnetic transient simulations," *IEEE Transactions on Power Apparatus and Systems*, vol. PAS-101, no. 1, pp. 147–157, Jan 1982.

[12] E. O. Schweitzer, B. Kasztenny, and M. V. Mynam, "Performance of time-domain line protection elements on real-world faults," in *42nd Annual Western Protective Relay Conference*, October 2015.

[13] *SynchroWAVe Event Software Instruction Manual*, Schweitzer Engineering Laboratories, 2018.

[14] A. Guzmán, G. Smelich, Z. Sheffield, and D. Taylor, "Testing traveling-wave line protection and fault locators," in *Conference on Developments in Power System Protection*, March 2018.